Research on Engineering Structures & Materials
www.jresm.org
Research Group

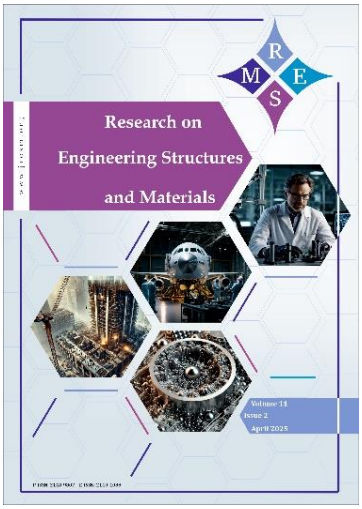

Experimental study on anisotropic mechanical properties of 3D reinforced concrete with discrete polyethylene fibers

Loan Thi Pham, Thi Hoai Thu Nguyen, Jie Yi Huang

Online Publication Date: 10 June 2025

URL: http://www.jresm.org/archive/resm2025-785me0326rs.html
DOI: http://dx.doi.org/10.17515/resm2025-785me0326rs

Journal Abbreviation: *Res. Eng. Struct. Mater.*

To cite this article
Pham L T, Nguyen T H T, Huang J Y. Experimental study on anisotropic mechanical properties of 3D reinforced concrete with discrete polyethylene fibers. *Res. Eng. Struct. Mater.*, 2025; 11(6): 3225-3244.

Research on Engineering Structures & Materials
www.jresm.org
MIM Research Group

Research Article

Experimental study on anisotropic mechanical properties of 3D reinforced concrete with discrete polyethylene fibers

Loan Thi Pham [*,1,a], Thi Hoai Thu Nguyen [1,b], Jie Yi Huang [2,c]

[1]*Faculty of Engineering and Technology, Haiphong University, Haiphong, Vietnam*
[2]*College of Civil Engineering and Architecture, Shandong University of Sciences and Technology, Qingdao, China*

Article Info

Article History:

Received 26 Mar 2025

Accepted 06 June 2025

Keywords:

Anisotropic mechanical properties;
Cracking pattern;
Flexural strength;
Compressive strength;
3D reinforced concrete;
Polyethylene fibers

Abstract

The mechanical properties of 3D-printed concrete, a key area of interest in civil engineering and materials science, are influenced by the loading orientation relative to the direction of the filament layer. This study investigates the mechanical behavior of 3D-printed reinforced concrete with discrete fibers—Polyethylene (PE) and High-Modulus Polyethylene (HPE)—under axial compression and flexural loading. Thirty-six printed and 21 molded specimens were analyzed to assess their flexural and compressive strengths, as well as the resulting cracking patterns that occurred. The results reveal that molded specimens exhibit greater strength than their printed counterparts. Additionally, strengths in the Z orientation exceed those in the Y orientation, with particularly pronounced differences observed in the Z direction. The optimal fiber content for PE and HPE reinforcement in printed concrete is determined to be 0.5%. This study enhances the understanding of fiber-reinforced concrete components and presents a comprehensive design framework that encompasses mix design, experimental procedures, and crack pattern analysis, focusing on both flexural and compressive strength.

1. Introduction

Concrete is inherently brittle and weak in tension, making it susceptible to sudden failures. Integrating high-tensile reinforcement materials is crucial for enhancing strength and preventing these failures. For centuries, builders have incorporated fibers such as straw and animal hair into mortar and bricks to enhance their tensile properties [1]. This established technique highlights the importance of innovative materials in producing safer and more durable concrete structures. Incorporating reinforcement in 3D-printed concrete structures poses a significant challenge in this field. A promising solution to the reinforcement issue is replacing traditional steel bars with short fibers [2, 3]. This approach streamlines the reinforcement process and enhances the material properties of concrete. Fiber-reinforced cement-based materials are needed to broaden the applications of 3D-printed concrete in designing high-performance structures. These materials can significantly improve mechanical properties, making structures more resilient and durable, while effectively addressing issues related to brittleness and cracking.

Reinforcing concrete with short, discontinuous fibers presents a groundbreaking approach to enhancing the performance of the concrete matrix during mixing. This innovative technique significantly boosts the mechanical properties of concrete, particularly its tensile strength, ductility, and durability, while reducing the risk of cracking. Various fiber types have been thoroughly examined for their potential as discrete reinforcement, providing multiple benefits. In

*Corresponding author: loanpt80@dhhp.edu.vn
[a]orcid.org/ 0000-0001-7081-0285; [b]orcid.org/0009-0000-9385-538X; [c]orcid.org/ 0000-0002-8377-214X
DOI: http://dx.doi.org/10.17515/resm2025-785me0326rs

the pursuit of improving the mechanical properties of cementitious matrices, four primary categories of fiber materials have emerged from extensive testing, each presenting remarkable advantages, as listed in Table 1.

Table 1. Types of fibers used in concrete by category, with select properties [4]

	Metalic			Glass				Natural	
	Steel	Stainless Steel		Silica Glass	Basalt Glass	GFRP/BFRP*		(Sect. 6 for Details)	
Tensile Strength (MPa)	1700	1030		1700 - 4600	1800 - 4800	1080		70 - 2000	
Elastic Modulus (GPa)	200	200		72 - 89	72 - 110	44		1.0 - 85	
Ultimate Elongation (%)	0.5 - 3.5	0.5 - 3.5		2.0 - 3.5	2.0 - 3.5	2.0 - 3.0		2.0 - 30.0	
Water Absorption (%)	-	-		-	-	-		High	
Specific Gravity	7.84	7.8		2.6 - 2.7	2.55 - 2.8	1.9 - 2.1		1 - 1.5	
	Synthetic								
	Polypropylene	Polyolefin	Polyethylene	Polyester	PVA**	Carbon	Nylon	Acrylic	Aramid
Tensile Strength (MPa)	60 - 700	300 - 700	40 - 3000	250 - 1000	850 - 1600	1500 - 7000	300 - 950	300 - 1000	2300 - 3400
Elastic Modulus (GPa)	1.5 - 10	3.0 - 10	0.5 - 120	10 - 20	25 - 41	30 - 500	3.0 - 5.4	3.8 - 17	70 - 143
Ultimate Elongation (%)	8.0 - 15.0	5.0 - 15.0	3.0 - 80.0	10.0 - 50.0	5.0 - 7.0	0.5 - 2.5	10.0 - 20.0	7.5 - 50.0	2.0 - 4.5
Water Absorption (%)	-	-	-	0.2 - 0.6	0.1 - 1.0	-	2.5 - 5.0	1.0 - 2.5	1.2 - 4.0
Specific Gravity	0.9 - 0.95	0.9 - 0.95	0.92 - 0.98	1.32 - 1.38	1.3	1.6 - 1.9	1.13 - 1.15	0.91 - 1.2	1.39 - 1.47

* GFRP = Glass Fiber Reinforced Polymer; BFRP = Basalt Fiber Reinforced Polymer; ** PVA = Polyvinyl Alcohol

Early studies on concrete 3D printing primarily focused on mix design and the rheological characteristics essential for effective process management [5-8]. Following this, research shifted to exploring the mechanical behavior of printed concrete components. Numerous investigations have revealed that 3D printable concrete exhibits anisotropic behavior, with compressive and flexural strengths evaluated in various loading directions [9-13]. However, inconsistencies in the findings emerged, indicating that the mechanical properties vary based on the mix type, printer system, and specific print parameters used in each study [14-15]. This variability highlights the complexities in understanding the mechanical behavior of 3D printed concrete and emphasizes the need for further research to establish consistent conclusions across diverse methodologies and materials. Moreover, few studies have concentrated on developing fiber-reinforced cement-based materials suitable for 3D printing. While extensive research has been conducted on various reinforcement methods in traditional concrete, the unique challenges of 3D printing require innovative strategies that blend both material properties and the printing process [16-17]. The potential of fiber reinforcement to enhance the mechanical characteristics of 3D-printed concrete is a promising area for future exploration, particularly regarding how different types and configurations of fibers influence the performance of the final printed structure. Such research could significantly advance 3D printing in construction, leading to safer and more durable structures.

The review highlights an increasing interest in fiber-reinforced, extrusion-based 3D printing concrete, which is crucial for enhancing the practical applications of the future. Nevertheless, most existing research primarily concentrates on selecting and optimizing additives, fibers, and cement, as well as evaluating the workability and rheological characteristics of these innovative materials [8, 12, 18]. This focus on individual components creates a notable gap in systematic studies regarding how fibers influence the anisotropic properties of 3D-printed cement-based materials.

Fiber-reinforced concrete (FRC) has become a prominent material in civil engineering due to its notable benefits, such as (1) strength in both compressive and flexural bending assessments, (2) enhanced tensile strength, (3) increased durability, and (4) superior energy absorption [19]. Fibrous reinforcement is cost-effective as it shortens installation time compared to traditional techniques. FRC is beneficial because fibers are pre-mixed into the concrete, facilitating its application across various engineering fields. Recent research examines the impact of fibers on mechanical properties, such as residual strength, tensile splitting strength, and flexural strength, especially following heat exposure [20-22]. Polypropylene (PP), polyethylene (PE), and glass fiber (GF) are recognized for their affordability, lightweight nature, corrosion resistance, toughness, and resistance to shrinkage cracking. These synthetic fibers are gaining popularity in concrete reinforcement to enhance its mechanical properties. Fig. 1 illustrates the fibers selected and their recommended amounts for this study.

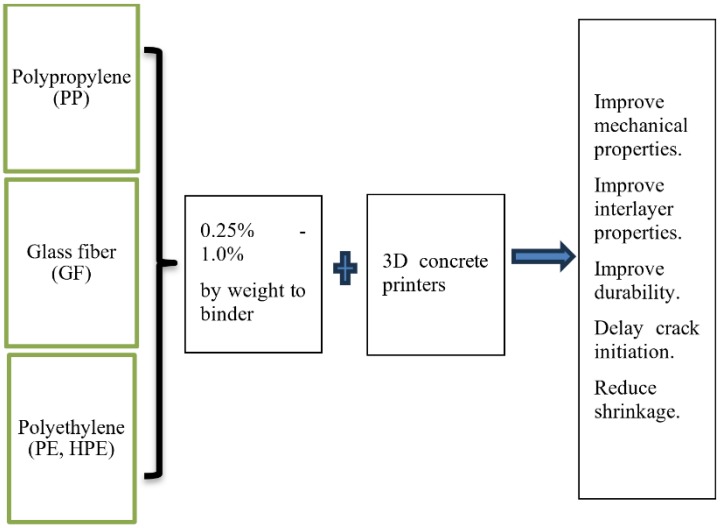

Fig. 1. Recommended fibers and effectiveness

The authors focus on uncovering the anisotropic mechanical properties of 3D-reinforced concrete, which incorporates discrete fibers including Polyethylene (PE) and High-Modulus Polyethylene (HPE). The authors investigated 36 printed specimens alongside 21 molded specimens to evaluate the flexural strengths, followed by assessments of the compressive strengths of the 3D-printed concrete. Addressing this gap is essential as it fosters a deeper understanding and optimization, ultimately enhancing the resilience and performance of 3D-printed concrete structures in real-world applications.

2. Experimental Program

2.1. Materials

This research selected ordinary Portland cement from Chiffon PC40 and fly ash [23] sourced from the Haiphong thermal power plant as binder components. This combination enhances the mechanical properties of our 3D-printed concrete, promoting sustainability. Incorporating fly ash improves workability and significantly increases the concrete's strength and durability while mitigating the environmental impact of cement production [24].

This study used commercially available manufactured natural sand with a nominal maximum aggregate size of 1.5 mm, in conjunction with crushed sand featuring a nominal maximum aggregate size of 2.5 mm. The selection of these specific aggregate sizes was crucial for assessing the mechanical properties of the 3D-printed concrete, as the size and type of aggregates significantly impact the overall performance and strength characteristics of the concrete mix. Additionally, ViscoCrete 3000-200M, a high-performance superplasticizer, plays a crucial role in enhancing the workability of fresh concrete. This additive dramatically enhances fluidity, facilitating easier placement and ensuring superior compaction without compromising strength. The physical properties of these ingredients are listed in Table 2.

Table 2. Properties of binder and aggregates

Material	Density (kg/m^3)	Sieve size (mm)
Cement (Chiffon PC40)	2.98	0.08
Fly ash (Haiphong Thermal Power Plant)	2.02	0.08
Natural sand (Lo River)	1.41	1.25
Crushed sand (Ha Nam Province)	1.405	2.5

Polyethylene (PE) and High-Modulus Polyethylene (HPE) were used in varying ratios. The properties of the fibers are given in Table 3.

Table 3. Properties of fibers

Properties	PE[25]	HPE[26]
Tensile strength (MPa)	520	3200
Modulus (GPa)	4.7	130
Diameter (mm)	0.032	0.0156
Length (mm)	12	12
Density (kg/m^3)	930	970

Fig. 2 illustrates the ingredients of fiber concrete. This representation showcases the various materials used in its composition, highlighting their proportions and the role each ingredient plays in enhancing the overall performance of the concrete.

Fig. 2. Ingredients of fiber concrete

The performance of a printed structure relies on maintaining the process under various conditions. The mixture comprises binders, admixtures, fine aggregates, and fibers. The effectiveness of a concrete mix is influenced by the materials employed, their proportions, strength, and bonding within the matrix, which affects both fresh and hardened properties [27]. In 3D-printed concrete, the printing open time, or setting time, indicates how long the material stays workable. This duration is critical for assessing performance, as it impacts the buildability and extrudability of the mixtures. A more extended setting improves fluidity and extrudability, while a shorter time provides adequate early strength. It can be summarized as shown in Fig. 3.

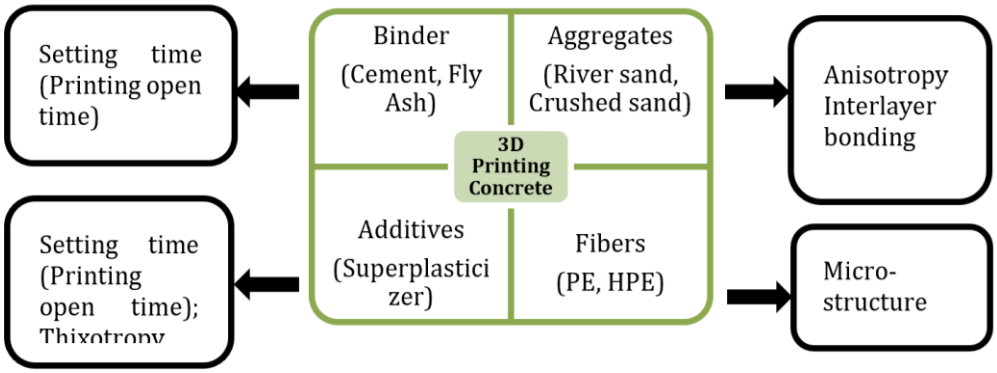

Fig. 3. Constituent material roles in the concrete matrix

After analyzing the constitutional materials, the authors employed a mixed design process, as presented in Fig. 4 [5], to determine the proportions of each material as given in Table 4. The slump test for each proportion yielded similar results, with slump values ranging from 9 mm to 13 mm, as shown in Fig. 5. Due to their highly thixotropic and low-workability characteristics, cementitious materials are typically designed for 3D printing applications. A mini-slump test was employed instead of the standard method, which is increasingly adopted in the literature for characterizing fresh 3D printable concrete. This approach omits tamping and utilizes a smaller cone to minimize disturbance to the internal structure of the material, thereby providing a more representative measure of flowability for printable mixes. While not governed by a formal standard, the procedure aligns with methodologies reported in recent studies [28]. The fresh and hardened states depicted in Fig. 5 were intended to provide a comprehensive understanding of the material's behavior at various stages of development. The slump test was performed on the fresh mix, while the hardened specimens were shown for visual comparison after curing.

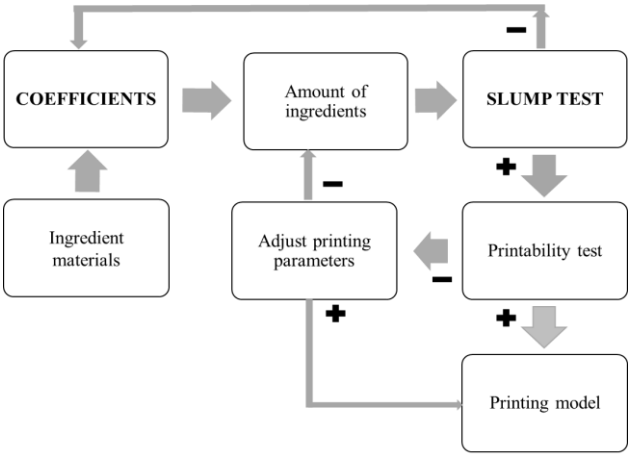

Fig. 4. Mix proportion design process

PE-0.25

PE-0.50

PE-0.75

HPE-0.25

HPE-0.50

PC-00

Fig. 5. Slump test results

Table 4. Mix proportions

Mix Label	Cement	Fly Ash	Water	Natural sand	Crushed sand	Fiber (%)	SP (%)
PE-0.25 HPE-0.25	0.75	0.25	0.32	0.375 (1.25mm)	1.125 (2.5mm)	0.25	0.4
PE-0.5 HPE-0.5	0.75	0.25	0.32	0.375 (1.25mm)	1.125 (2.5mm)	0.50	0.4
PE-0.75 PC-00	0.75	0.25	0.32	0.375 (1.25mm)	1.125 (2.5mm)	0.75 0.00	0.4

(Note: Binder = Cement and Fly Ash; values in Table are ratios of each ingredient to binder weight)

2.2. Printing Specimens

As per TCVN 3119: 2022, titled "Hardened Concrete – Test Method for Flexural Tensile Strength" [29], the specimens measure 280 mm in length, 70 mm in width, and 70 mm in height. A circular nozzle with a 25 mm diameter was used to print all components. Each printing layer has a height of 10 mm, with filament widths varying from 32 mm to 35 mm. In total, 36 specimens were printed, as illustrated in the accompanying figure. However, the specimens with an HPE fiber ratio of 0.75 could not be printed successfully due to a blockage in the print head, as illustrated in Fig. 6.

(a) Printed specimens

(b) Blockage of HPE-0.75 specimen

Fig. 6. Printing specimens

Fig. 7. Molded specimens

At the same time, reference specimens were carefully prepared with the same mix ratio. These specimens were designed to maintain consistency within the experimental setup, thereby facilitating accurate comparisons and evaluations. Each specific fiber ratio had three specimens, as

illustrated in Fig. 7. According to TCVN 3121-11:2022, titled "Mortar for masonry - Test methods, Part 11: Determination of flexural and compressive strength of hardened mortars" [30], the specimens measured 160 mm in length, 40 mm in width, and 40 mm in height. This experimental arrangement enables a thorough examination of how different fiber ratios impact the flexural performance of the materials, allowing for an in-depth comparison of the three-dimensional printed samples with those produced through traditional casting methods. All specimens were effectively cured at room temperature after printing and maintained in this condition until the 28th day, ensuring their optimal quality and performance.

2.3. Flexural Test

The flexural test indirectly assesses the tensile strength of materials. This test measures a specimen's ability to resist failure under bending. Flexural strength represents the maximum stress the material can endure at the point of rupture. It is also called bend strength, fracture strength, or modulus of rupture. This testing method provides a systematic approach for evaluating the flexural strength of concrete using a simple beam subjected to center-point loading, as illustrated in Fig. 8. It complies with the standards established in TCVN 3119: 2022 and TCVN 3121-11: 2022, ensuring dependable and consistent outcomes in the assessment of material performance.

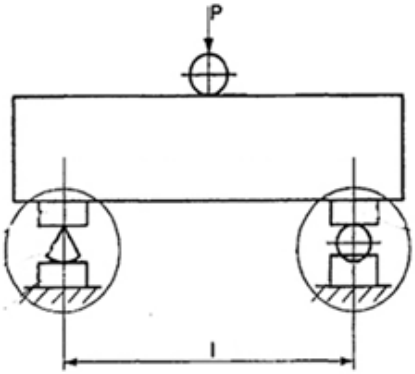

(a) Flexural test scheme

(b) Test machine YE200C

8c) Printed sample flexural test

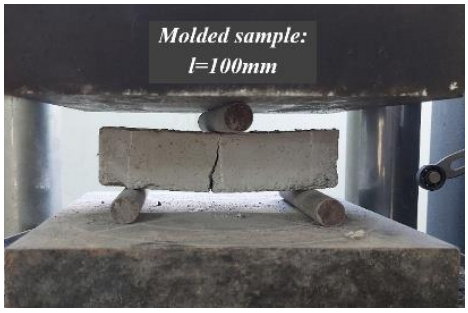

(d) Molded sample flexural test

Fig. 8. Flexural test

2.4. Compression Test

Following the completion of the bending tests, which failed the printed specimens, compression tests were conducted using the remaining halves of each specimen. The steel plate dimensions are 70x70mm for printed specimens and 40x40mm for molded specimens, as shown in Fig. 9. This approach ensured that we utilized every piece effectively while gaining insights into their structural integrity under different stress conditions. The compression tests adhered strictly to the prescribed procedures and loading protocols outlined in the Vietnam standards. This compliance guarantees that the testing process is valid and reliable, ensuring accurate and meaningful results. Details of the testing setup and methodology can be seen in the accompanying documentation [30].

(a) Compressive test scheme (b) Printed specimen (c) Molded specimen

Fig. 9. Compression test

3. Anisotropic Mechanical Properties – Results and Discussions

3.1. Cracking Pattern

Initially, flexural tests were performed, revealing two distinct cracking patterns regardless of the loading direction, whether X or Y. The printed and molded specimens without fibers exhibited entirely brittle failures, fracturing into two separate pieces, as illustrated in Fig. 10 (a, c). This behavior is typical of unreinforced materials, where cracks propagate rapidly and cause complete separation upon reaching the ultimate load. In contrast, the specimens reinforced with fibers demonstrated cracking up to the ultimate load without complete separation, as illustrated in Fig. 10 (b, d). The introduction of fibers significantly altered the failure mode, preventing complete fracture and instead promoting controlled cracking that maintained the specimen's structural integrity. These findings are consistent with previous research on fiber-reinforced concrete, where fibers contribute to bridging cracks and delaying failure under flexural loads [31], [32] . This improvement in the failure mechanism is attributed to the fibers' ability to distribute the stress more evenly across the material, reducing the likelihood of catastrophic fracture.

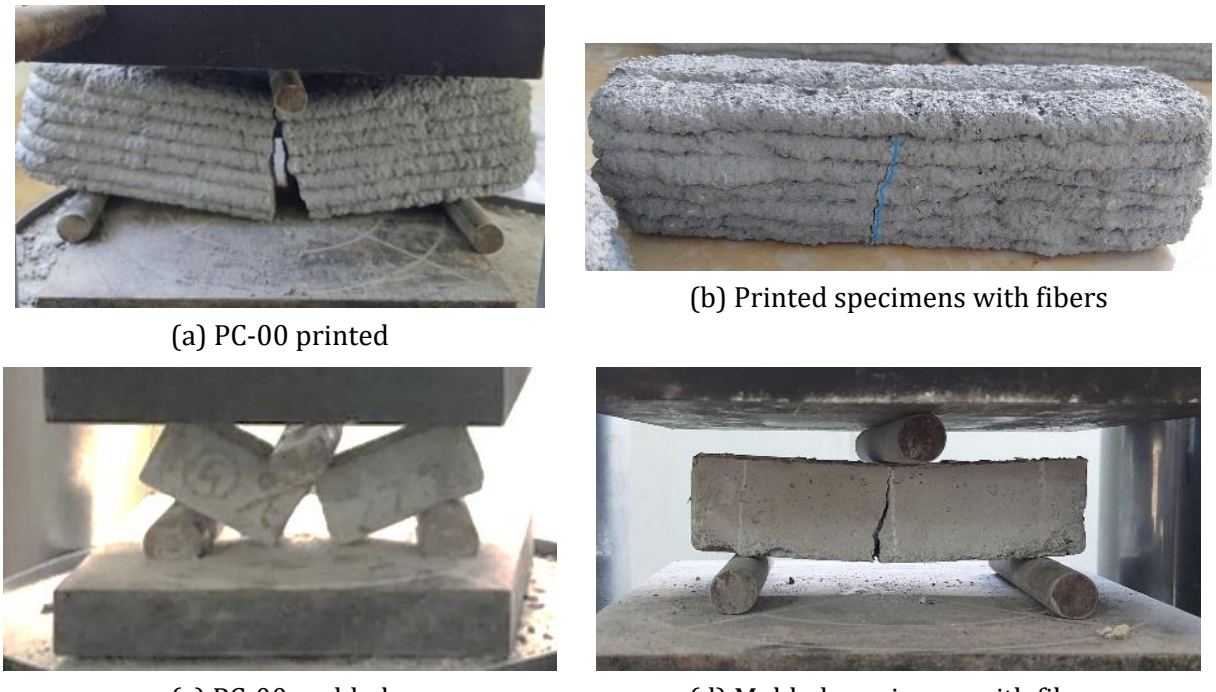

(a) PC-00 printed (b) Printed specimens with fibers

(c) PC-00 molded (d) Molded specimens with fibers

Fig. 10. Flexure cracking patterns

The strategic integration of fibers into the composite has significantly enhanced its structural integrity, as evidenced by the marked absence of crack propagation along the interfaces between the filaments. The observed enhancement in cracking patterns due to fiber reinforcement suggests that the incorporation of fibers not only improves the material's load-bearing capacity but also modifies the fracture behavior, making it more suitable for applications requiring durability and toughness. The interfacial bonding between the fibers and the matrix plays a crucial role in this behavior, particularly in 3D-printed materials, where layer interfaces are typically weaker [31], [32]. In this study, the fibers contributed to overcoming these inherent weaknesses, improving the overall performance of the composite. Following the flexural tests, compressive tests were performed on the fractured halves of the specimens. The results revealed that the specimens without any fiber reinforcement from both types experienced considerable crushing, as shown in Fig. 11 (h). This observation is indicative of the brittle nature of the unreinforced material, which failed under compressive stress due to the lack of crack control.

(a) Printed specimens with fibers

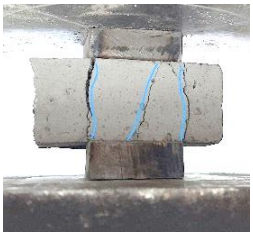

(b) Molded specimens with fibers

(c) PE-0.25

(d) PE-0.5

(e) PE-0.75

(f) HPE-0.25

(g) HPE-0.5

(h) Printed and molded without fibers

Fig. 11. Compression cracking patterns

Interestingly, the cracking patterns observed in both the printed and molded specimens displayed a tendency toward an inclined crack configuration, as depicted in Fig. 11 (a, b). This type of cracking is commonly observed in materials that fail under compressive stress, where internal forces result in diagonal shear failure. Notably, the specimens reinforced with high-performance engineered (HPE) fibers exhibited a superior capacity to maintain their shape and structural integrity after the application of the ultimate load, as shown in Fig. 11 (f, g). In contrast to those reinforced with polyethylene (PE) fibers, which faced more significant deformation, as shown in Fig. 11 (c, d). This distinction highlights the superior performance of HPE fibers in enhancing the material's mechanical properties, particularly under compressive stress. The better shape retention of HPE-reinforced specimens suggests that these fibers provide superior crack-bridging and stress distribution capabilities compared to PE fibers, which may have less effective bonding with the matrix. The differences in performance between HPE and PE fibers emphasize the importance of fiber type in determining the overall material properties, particularly when used in 3D-printed

concrete. These findings underscore the significance of fiber reinforcement, particularly HPE fibers, in improving both the flexural and compressive strength of 3D-printed concrete. The ability of HPE fibers to maintain structural integrity and delay failure under stress represents a significant advancement in material design for additive manufacturing in construction applications.

3.2. Flexural Strength

Using the ultimate load values obtained from each test, the flexural strength of the specimens was calculated with Equation (1).

$$\sigma = \frac{M}{W} = \frac{P.l}{4.(\frac{b.a^2}{6})} = 1{,}5.\frac{P.l}{a^3} \quad (1)$$

Where, σ is the flexural strength of the specimen (MPa); P is the ultimate load value (N); l is a clear span; 210 (mm) for printed and 100 (mm) for molded specimens; a is the dimension of the cross-section; taken 70 (mm) for printed and 40 (mm) for molded specimens. The results of the flexural strengths are given in Table 5, Table 6, and Table 7.

Table 5. Flexural strength of PE fibers reinforced printed and molded specimens.

Specimens	Dimension (mm)	Fiber ratio (%)	Type	Loading orientation	Failure load (kN)	Span length (mm)	Flexural Strength (MPa)
PE-0.25	280x70x70	0.25	Printed	Z	7.81	210	7.17
PE-0.5	280x70x70	0.5	Printed		7.55	210	6.93
PE-0.75	280x70x70	0.75	Printed		7.27	210	6.68
PE-0.25	280x70x70	0.25	Printed	Y	6.97	210	6.41
PE-0.5	280x70x70	0.5	Printed		7.31	210	6.72
PE-0.75	280x70x70	0.75	Printed		7.21	210	6.62
PE-0.25	160x40x40	0.25	Molded	Z, Y	3.08	100	7.22
PE-0.5	160x40x40	0.5	Molded		3.18	100	7.45
PE-0.75	160x40x40	0.75	Molded		3.14	100	7.35

Table 6. Flexural strength of HPE fibers reinforced printed and molded specimens

Specimens	Dimension (mm)	Fiber ratio (%)	Type	Loading orientation	Failure load (kN)	Span length (mm)	Flexural Strength (MPa)
HPE-0.25	280x70x70	0.25	Printed	Z	8.14	210	7.48
HPE-0.5	280x70x70	0.5	Printed		8.99	210	8.26
HPE-0.25	280x70x70	0.25	Printed	Y	7.35	210	6.75
HPE-0.5	280x70x70	0.5	Printed		8.77	210	8.05
HPE-0.25	160x40x40	0.25	Molded	Z, Y	16.67	100	7.59
HPE-0.5	160x40x40	0.5	Molded		3.70	100	8.67
HPE-0.75	160x40x40	0.75	Molded		3.94	100	9.23

Table 7. Flexural strength of printed and molded specimens without fibers

Specimens	Dimension (mm)	Fiber ratio (%)	Type	Loading orientation	Failure load (kN)	Span length (mm)	Flexural Strength (Mpa)
PC-00	280x70x70	0	Printed	Z	1.41	210	6.93
	280x70x71	0	Printed	Y	1.29	211	6.36
	160x40x40	0	Molded	Z, Y	2.98	100	6.98

The Z loading orientation refers to being perpendicular to the filament's surface. On the other hand, the Y loading orientation indicates the direction parallel to the filament's surface, as shown in Fig.

12. The flexural strength results summarized in the tables above can be used to construct comparative diagrams illustrating the performance differences among specimens.

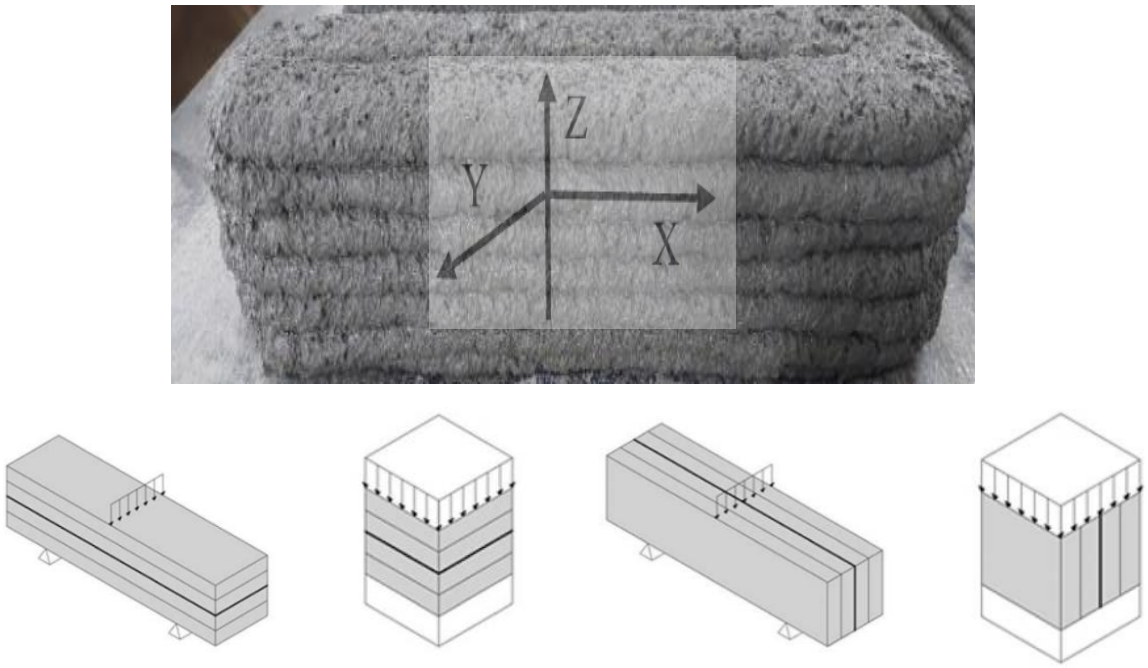

(a) Z loading orientation (b) Y loading orientation

Fig. 12. Loading orientation

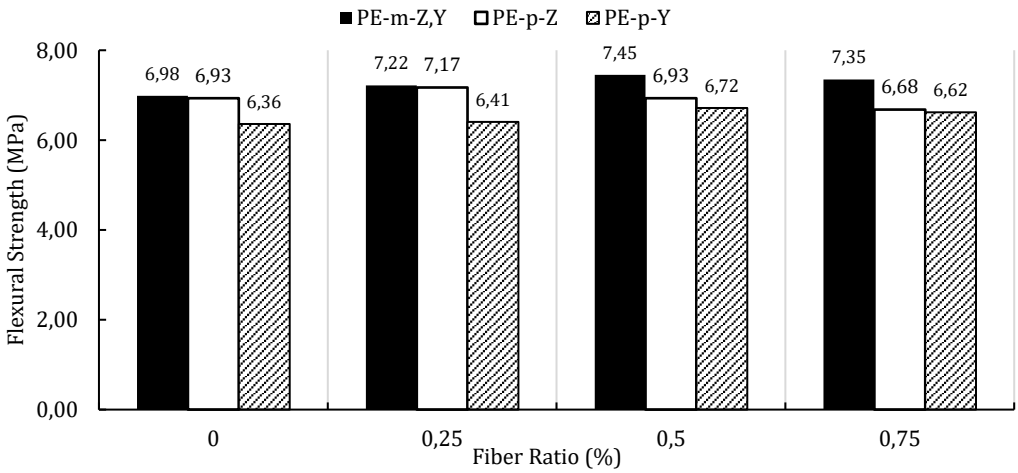

Fig. 13. Flexural strength of printed and molded specimens with variations of PE fibers. *(Note: "m" refers to "molded"; "p" refers to "printed")*

As illustrated in Fig. 13, the flexural strength of 3D-printed specimens under Z-direction loading consistently exceeds that observed under Y-direction loading across all fiber contents. The highest strength in the Z-direction is 7.17 MPa at a fiber content of 0.25%, whereas the Y-direction reaches a maximum of 6.72 MPa at 0.5% fiber content. The disparity in strength between the two loading orientations diminishes with increasing fiber dosage. These findings indicate that the optimal fiber content ranges between 0.25% and 0.5%, as further additions lead to a reduction in mechanical performance. Relative to the unreinforced control group, the inclusion of PE fibers yields modest improvements in flexural strength: a 3.5% increase for PE-0.25 specimens in the Z-direction and a 5.6% increase for PE-0.5 specimens in the Y-direction. Nonetheless, the flexural strength of printed specimens remains approximately 10% lower than that of conventionally cast counterparts. This difference is partially attributed to variations in specimen dimensions (280×70×70 mm for printed

versus 160×40×40 mm for molded) and testing spans (210 mm versus 100 mm), which have been duly accounted for in the analysis using standard procedures for flexural and compressive strength evaluation, as prescribed by relevant codes and literature. It is essential to note that the primary objective of this study was not to conduct a direct 1:1 comparison of the intrinsic material properties between printed and molded specimens, but rather to investigate relative trends in performance influenced by fiber type and print orientation under controlled and consistent preparation and testing conditions. Nonetheless, the authors acknowledge that size effects may influence absolute strength values.

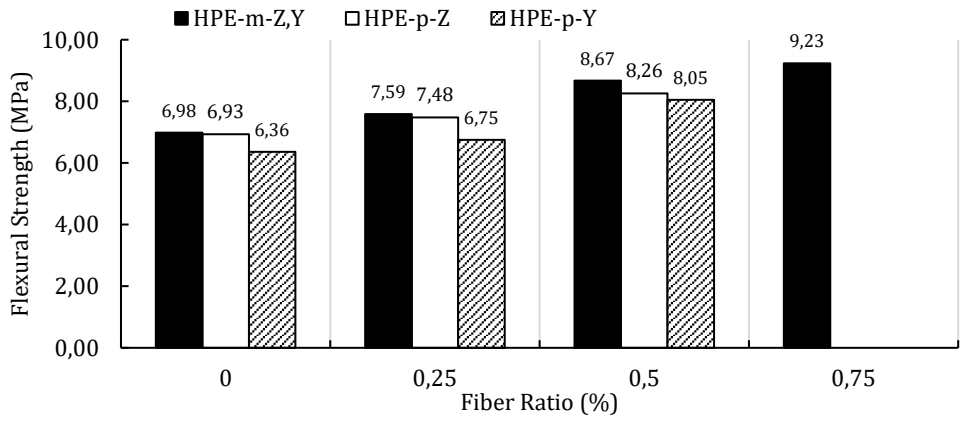

Fig. 14. Flexural strength of printed and molded specimens with variations of HPE fibers

As illustrated in Fig. 14, the flexural strength of printed specimens under Z-direction loading consistently exceeds that under Y-direction loading across all fiber ratios. The highest flexural strengths recorded are 8.26 MPa in the Z-direction and 8.05 MPa in the Y-direction, both corresponding to a fiber content of 0.5%. The results indicate a positive effect of HPE fiber reinforcement, with strength increasing significantly as fiber content rises. Specifically, the HPE-0.5 specimens exhibit improvements of 19% and 27% in the Z and Y directions, respectively, compared to unreinforced printed samples (PC-00). However, the specimen with 0.75% fiber content encountered printing issues due to nozzle blockage. Despite this, the overall trend indicates a consistent increase in flexural strength with the addition of fiber. Nevertheless, the flexural performance of all printed specimens remains slightly lower than that of molded specimens, with reductions of up to 4.8% in the Z-direction and 11% in the Y-direction. This difference is also partially attributed to variations in specimen dimensions (280×70×70 mm for printed versus 160×40×40 mm for molded) and testing spans (210 mm versus 100 mm).

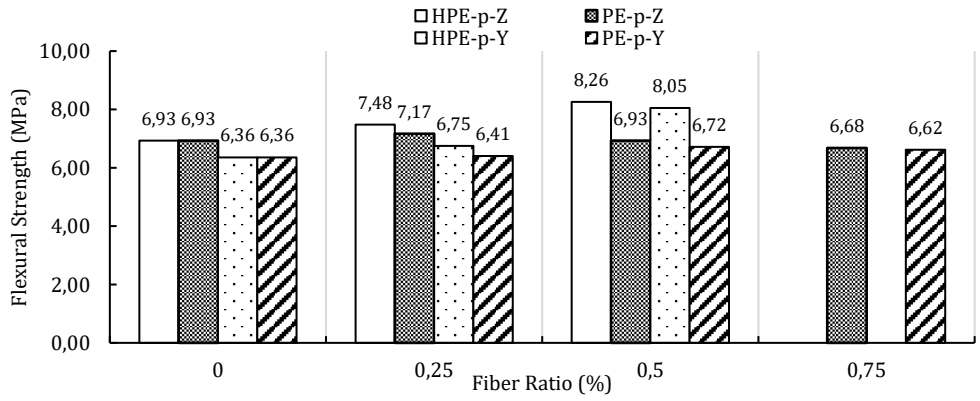

Fig. 15. Flexural strength comparison between HPE and PE fiber of printed specimens

The use of HPE fiber significantly enhances flexural strength compared to PE fiber. Specifically, printed specimens exhibit increased flexural strength up to 20% in both the Z and Y loading orientations. This improvement is primarily attributed to the mechanical properties of HPE fiber, which are considerably superior to PE fiber in terms of tensile strength and modulus, as

demonstrated in Table 1. These findings are visually depicted in Fig. 15, showcasing the exceptional mechanical properties of HPE fiber under various loading conditions. This enhancement in performance suggests that HPE fiber could be a more advantageous option for applications that require higher-strength materials.

The incorporation of HPE fibers significantly improves the flexural strength of printed specimens compared to those reinforced with conventional PE fibers. In both Z and Y loading orientations, flexural strength increases by up to 20%. This enhancement is primarily attributed to the superior mechanical characteristics of HPE fibers, particularly their higher tensile strength and elastic modulus, as presented in Table 3. Fig. 15 further illustrates the enhanced performance of HPE fibers under various loading conditions. These results suggest that HPE fiber offers a more effective reinforcement solution for applications demanding higher structural performance. Several key findings emerged from the investigation of flexural strength:

- HPE fibers significantly enhance the flexural strength of both printed and molded specimens by up to 27%, while PE fibers yield a modest improvement of less than 5.6%.
- Flexural strength in printed specimens remains consistently lower than in molded counterparts across both Z and Y loading orientations.
- PE fibers demonstrate optimal performance at concentrations between 0.25% and 0.5%, within which notable gains in flexural strength are observed.
- While increased HPE fiber content markedly improves flexural performance, careful control of material flow is essential to avoid nozzle clogging during 3D printing.
- In both fiber-reinforced systems, specimens loaded in the Z-direction generally exhibit higher flexural strength than those in the Y-direction. However, both remain inferior to molded specimens at equivalent fiber ratios.
- Due to their superior mechanical properties, HPE fibers offer approximately 20% higher flexural strength than PE fibers, making them a preferred reinforcement for applications requiring enhanced structural capacity.

Extensive research on the mechanical behavior of 3D-printed cement-based materials consistently reveals significant anisotropy after hardening. This phenomenon has been widely reported in the literature. Unlike traditional molded specimens, which typically exhibit isotropic properties, 3D-printed elements display marked variations in strength, stiffness, and other mechanical properties depending on layer orientation. The layer-by-layer deposition process introduces inherent heterogeneity, resulting in directional dependencies that significantly impact structural performance under load. A thorough understanding of this anisotropic behavior is crucial for accurately predicting the mechanical response of 3D-printed structures, underscoring the importance of carefully considering printing orientation and design parameters in cement-based additive manufacturing. This anisotropic behavior aligns with findings from previous studies [9], [11], [33], [34], which reported that 3D printing induces directional dependencies in material properties. Understanding this anisotropy is crucial for accurately predicting the performance of 3D-printed structures in real-world conditions. For example, structures subjected to loading in the Z-direction often exhibit superior mechanical performance compared to those loaded in the Y-direction, primarily due to more uniform interlayer bonding and a reduction in weak interfaces along the build direction.

In the additive manufacturing process, voids and weak contact interfaces often form between adjacent filaments that are aligned parallel to the printing direction. These defects significantly compromise flexural performance, particularly under varied loading conditions. Under bending, the specimen's ultimate strength is primarily governed by the maximum tensile stress at the mid-span region. When loaded in the Y-direction, this tensile stress acts perpendicular to the layer interfaces, precisely where bonding is weakest due to limited interlayer fusion. Moreover, the effectiveness of fiber reinforcement is reduced, as continuous fibers often fail to adequately bridge the interfaces between printed layers, further diminishing structural integrity. This insufficient fiber penetration, coupled with poor interlayer adhesion and unfavorable stress orientation, leads to substantially lower flexural strength in the Y-direction compared to the Z-direction. These findings highlight the importance of enhancing interlayer bonding and optimizing filament

alignment to improve the structural performance of 3D-printed composites. Additionally, 3D-printed specimens exhibit consistently lower flexural strength than their molded counterparts. This disparity is primarily attributed to the layered architecture of printed elements, which introduces weak interfacial zones. In contrast, molded specimens benefit from a homogeneous material matrix that promotes greater strength and uniformity. As a result, both Z- and Y-direction loading of printed samples yields inferior flexural performance relative to molded specimens. These observations are in line with previous studies [35], [36], which reported significant mechanical degradation in 3D-printed cementitious materials due to anisotropy and inadequate interlayer bonding.

3.3. Compressive Strength

Using the ultimate load values obtained from each test, the compressive strength of the specimens was calculated with Equation (2):

$$\sigma = \frac{P}{A} \tag{2}$$

Where, σ is the compressive strength of the specimen (MPa); P is the ultimate load value (N); A is the area of the steel plate, taken as 70x70 mm for printed specimens and 40x40 mm for molded specimens. The results of compressive strengths are given in Table 8, Table 9, and Table 10.

Table 8. Compressive strength of PE fibers reinforced printed and molded specimens.

Specimens	Dimension (mm)	Fiber ratio (%)	Type	Loading orientation	Failure load (kN)	Plate Width (mm)	Compressive Strength (MPa)
PE-0.25	280x70x70	0.25	Printed	Z	113.29	70	23.12
PE-0.5	280x70x70	0.5	Printed		130.00	70	26.53
PE-0.75	280x70x70	0.75	Printed		119.11	70	24.31
PE-0.25	280x70x70	0.25	Printed	Y	53.69	70	10.96
PE-0.5	280x70x70	0.5	Printed		78.78	70	16.08
PE-0.75	280x70x70	0.75	Printed		67.65	70	13.81
PE-0.25	160x40x40	0.25	Molded	Z, Y	54.32	40	33.95
PE-0.5	160x40x40	0.5	Molded		60.58	40	37.86
PE-0.75	160x40x40	0.75	Molded		50.55	40	31.59

Table 9. Compressive strength of HPE fibers reinforced printed and molded specimens.

Specimens	Dimension (mm)	Fiber ratio (%)	Type	Loading orientation	Failure load (kN)	Span length (mm)	
HPE-0.25	280x70x70	0.25	Printed	Z	130.00	70	26.53
HPE-0.5	280x70x70	0.5	Printed		146.25	70	29.85
HPE-0.25	280x70x70	0.25	Printed	Y	54.74	70	11.17
HPE-0.5	280x70x70	0.5	Printed		85.18	70	17.38
HPE-0.25	160x40x40	0.25	Molded	Z, Y	56.89	40	35.56
HPE-0.5	160x40x40	0.5	Molded		62.02	40	38.76
HPE-0.75	160x40x40	0.75	Molded		51.73	40	32.33

Table 10. Compressive strength of printed and molded specimens without fibers

Specimens	Dimension (mm)	Fiber ratio (%)	Type	Loading orientation	Failure load (kN)	Span length (mm)	
PC-00	280x70x70	0	Printed	Z	81.93	70	16.72
	280x70x70	0	Printed	Y	28.84	70	7.93
	160x40x40	0	Molded	Z, Y	52.51	40	32.82

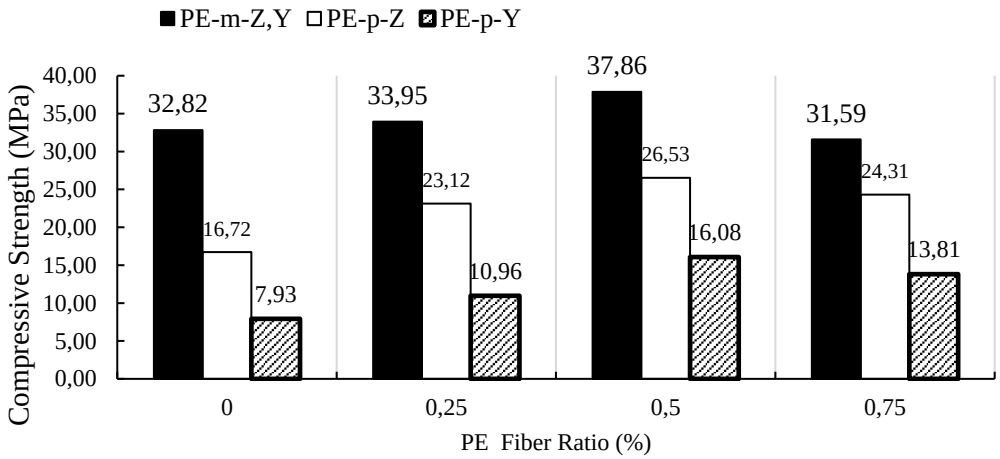

Fig. 16. Compressive strength of printed and molded specimens with variations of PE fibers

Fig. 16 illustrates that the compressive strength of printed specimens in the Z-direction is significantly higher than in the Y-direction. As the fiber ratio increases from 0% to 0.5%, the compressive strength rises from 16.72 MPa to a peak of 26.53 MPa in the Z-direction. Beyond this point, the strength declines to 24.31 MPa. This trend is also observed in the Y-direction, where the strength follows a similar pattern. The optimal fiber ratio is identified as 0.5%, as further increases in fiber content result in a reduced compressive strength. Notably, the addition of PE fibers significantly enhances compressive strength, with PE-0.5 printed specimens showing improvements of 58% and 103% in the Z and Y directions, respectively, compared to unreinforced specimens (PC-00 printed). Despite these gains, the compressive strength of the printed specimens remains much lower than that of molded specimens, with reductions of 31% in the Z-direction and 67% in the Y-direction at a 0.25% fiber ratio. The tolerance of printed specimens without fiber reinforcement is higher, with reductions of up to 49% and 82% in the Z and Y directions, respectively.

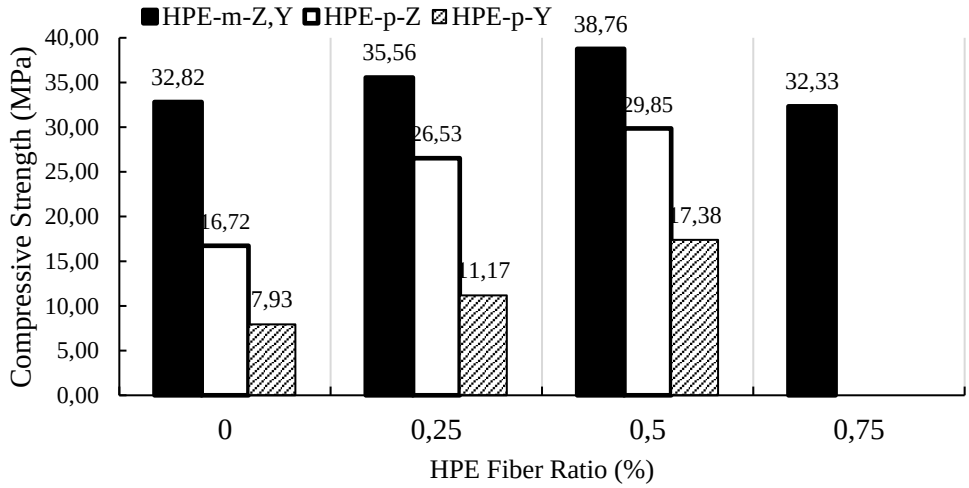

Fig. 17. Compressive strength of printed and molded specimens with variations of HPE fibers

The data presented in Fig. 17 shows that compressive strength in the Z-direction is significantly higher than in the Y-direction. As the fiber ratio increases from 0% to 0.5%, compressive strength rises from 16.72 MPa to a peak of 29.85 MPa in the Z-direction. Similarly, the compressive strength in the Y-direction follows a comparable trend, increasing from 5.88 MPa to 17.38 MPa. A notable trend emerges when analyzing printed specimens without fiber reinforcement, specifically with the incorporation of HPE fibers. The addition of HPE fibers substantially improves compressive strength, with specimens containing 0.5% HPE fibers (denoted as HPE-0.5 printed) showing improvements of 78% in the Z-direction and 120% in the Y-direction compared to the unreinforced

specimens (PC-00 printed). Despite these enhancements, printed specimens still exhibit significantly lower compressive strength than molded specimens, with reductions of 25% in the Z-direction and 68% in the Y-direction at a 0.25% material ratio. Consistent with observations for PE fibers, the results suggest that an optimal fiber ratio of 0.5% for HPE fibers yields the best compressive strength, with higher fiber content leading to a reduction in strength.

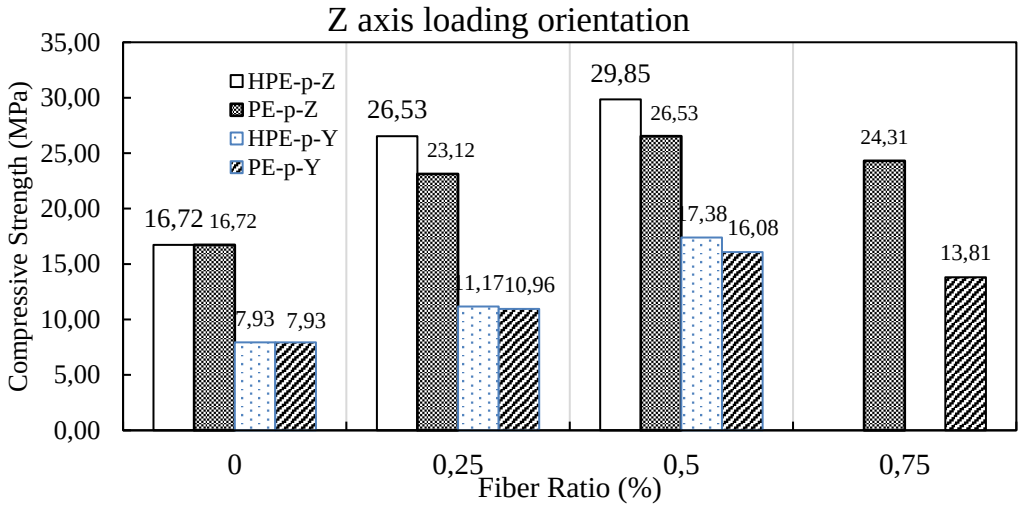

Fig. 18. Compressive strength comparison between HPE and PE fiber of printed specimens

The incorporation of HPE fibers significantly enhances compressive strength compared to PE fibers, as illustrated in Fig. 18. Specifically, printed specimens with 0.25% HPE fibers (HPE-0.25) show a 14.7% increase in compressive strength over their PE fiber counterparts (PE-0.25) in the Z-direction, and an 8.1% increase for specimens with 0.5% HPE fiber (HPE-0.5) compared to PE-0.5 in the Y-direction. In contrast, molded specimens only show a modest improvement of approximately 4%. These findings, visually represented in Fig. 18, underscore the superior mechanical properties of HPE fibers under various loading conditions. This enhancement suggests that HPE fiber is a more advantageous option for applications requiring high-strength materials. In terms of compressive strength, several notable conclusions can be drawn:

- Both PE and HPE fibers significantly enhance the compressive strength of both printed and molded specimens, demonstrating their effectiveness as reinforcement materials.
- The optimal fiber content for significantly improving compressive strength is 0.5% for both PE and HPE fibers.
- Testing results reveal that compressive strength is considerably higher in the Z-loading orientation compared to the Y-loading orientation for both types of fibers. However, it is essential to note that these strengths remain notably lower than those of molded specimens with equivalent fiber ratios, particularly in the Y-loading orientation.
- HPE fiber proves to be a more advantageous reinforcement for applications requiring high-strength materials. It outperforms PE fibers, providing a compressive strength increase ranging from 8.1% to 14.7%, thereby effectively enhancing structural performance.

Compressive strength demonstrates a pronounced anisotropy in 3D-printed specimens after hardening, more significant than that observed in flexural behavior. As illustrated in Fig. 19, the difference between Z and Y loading orientations becomes particularly evident under compressive loads. In the Y orientation, the load is applied parallel to the layer interfaces, which are inherently weaker due to insufficient interlayer bonding during the printing process. This configuration leads to premature failure, as crack propagation is facilitated along these weak interlaminar zones. As cracks initiate and spread, the filaments between the printed layers separate rapidly, causing sudden and brittle failure. This observation aligns with prior studies [37], [38], which also reported reduced compressive performance in the direction parallel to the printed layers due to poor interfacial adhesion.

Conversely, the Z loading orientation exhibits improved compressive strength because the applied load acts perpendicular to the layer interfaces, effectively mitigating the influence of interlaminar weaknesses. This behavior is analogous to that of molded specimens, which benefit from a more homogenous and continuous matrix structure. As a result, the compressive strength in the Z direction is closer to the performance of conventionally cast concrete. These findings underscore the significant impact of printing direction and layer bonding quality on the mechanical behavior of printed components. Moreover, they emphasize the need for enhanced printing strategies, such as optimized nozzle path planning, tailored mix designs, or post-treatment techniques, to improve interlayer adhesion and reduce anisotropy in structural applications of 3D-printed concrete.

Fig. 19. Cracking pattern in Y loading orientation

The compressive strength of 3D-printed specimens is substantially lower than that of conventionally molded specimens, with the difference being especially significant under the Y loading orientation. This reduction in strength is primarily attributed to the inherent characteristics of the additive manufacturing process, where material is deposited in successive layers. Such a process creates a laminated structure, leading to the formation of interfacial zones with relatively weak bonding between layers. When subjected to compressive loading in the Y direction, parallel to the interlaminar interfaces, these weak zones become critical points of failure, significantly compromising the specimen's ability to withstand load. Similar observations have been reported in earlier studies [39], where interlayer defects and voids have been found to contribute to the diminished compressive performance of printed concrete.

In contrast, molded specimens exhibit a more homogenous and monolithic internal structure due to the absence of layering, resulting in higher structural integrity and superior compressive strength. The uniform distribution of materials in molded samples allows them to resist compressive stress more effectively, particularly when compared to the anisotropic and heterogeneous nature of printed components. This performance gap between printed and molded specimens highlights the need to enhance interlayer bonding in 3D printing, potentially through the optimization of mix rheology, printing parameters, or post-processing techniques.

Moreover, the inclusion of fiber reinforcement, such as polyethylene (PE) or high-modulus polyethylene (HPE) fibers, has shown considerable potential in mitigating these weaknesses by bridging interfacial gaps and enhancing load transfer across layers. These findings highlight the significance of material design and structural optimization in enhancing the practical application of 3D-printed concrete in construction.

4. Conclusions

This research investigates the behavior of 3D-printed components under flexural and compressive loads, providing valuable insights into the impact of fiber reinforcement on material performance. Key findings and conclusions from the study are as follows:

- Effect of Fiber Reinforcement on Strength: The incorporation of HPE fibers significantly enhances both flexural and compressive strength of printed and molded specimens.

Specifically, HPE fibers improve the flexural strength by up to 27%, while PE fibers contribute a more minor improvement of less than 5.6%. Both fiber types significantly improve compressive strength, highlighting their effectiveness as reinforcement materials in 3D-printed concrete.

- Anisotropic Behavior of Printed Components: Testing results indicate that the flexural strength of printed specimens is typically higher in the Z loading orientation compared to the Y loading orientation. This anisotropic behavior, common in 3D-printed materials, is due to the layer-by-layer deposition process. However, despite this directional variation, the flexural strength of printed specimens remains lower than that of molded specimens with equivalent fiber ratios, particularly in the Y orientation.
- Optimal Fiber Ratios: The study identifies 0.5% as the optimal fiber ratio for achieving substantial improvements in compressive strength. Both PE and HPE fibers at this concentration show significant enhancements in material performance. Beyond this optimal ratio, increasing the fiber content does not lead to further improvements and may even cause a reduction in strength.
- HPE Fibers for High-Strength Applications: HPE fibers prove to be more advantageous for applications requiring higher-strength materials. Compared to PE fibers, HPE fibers offer a 20% increase in strength, making them a more effective choice for enhancing the structural performance of 3D-printed concrete.
- Challenges in Printing with High Fiber Content: While increasing the content of HPE fibers results in higher flexural strength, it is crucial to manage the material flow during the printing process to prevent nozzle blockages. This requires careful control over the printing parameters to ensure the consistency and quality of the printed components.

In conclusion, fiber reinforcement plays a crucial role in enhancing the mechanical properties of 3D-printed concrete. HPE fibers, in particular, offer significant improvements in strength, making them a promising option for high-performance applications. However, further optimization of printing processes and fiber content is necessary to address the challenges related to material flow and interlayer bonding.

Acknowledgements

The authors would like to express their sincere gratitude to the research group "Structural and Technology for Sustainable Construction" for their continuous support throughout this study. Special thanks are extended to Haiphong University in Vietnam for providing laboratory assistance. The authors also appreciate the VIDPOL Joint Stock Company for their development of the experimental equipment, and the Thanh Hung Concrete Joint Venture Company for their generous material support. Their contributions have been invaluable in enabling the successful completion of this research.

References

[1] Hejazi SM, Sheikhzadeh M, Abtahi SM, Zadhoush A. A simple review of soil reinforcement by using natural and synthetic fibers. Constr Build Mater. 2012 May;30:100-16. https://doi.org/10.1016/j.conbuildmat.2011.11.045

[2] Amiri FS, Baghdadi A, Kwon H. New Reinforcement Approach for Freeform Concrete Components through Carbon Fiber 3D Printing. In: Proceedings of the IASS 2024 Symposium: Redefining the Art of Structural Design. 2024. p. 1-15.

[3] Mohajerani A, et al. Amazing types, properties, and applications of fibres in construction materials. Materials (Basel). 2019;12(16):1-45. https://doi.org/10.3390/ma12162513

[4] Dopko M. Fiber reinforced concrete: Tailoring composite properties with discrete fibers [thesis]. Iowa State University; 2018.

[5] Pham LT, et al. Development of 3D printers for concrete structures: mix proportion design approach and laboratory testing. Smart Sustain Built Environ. 2022 Aug. https://doi.org/10.1108/SASBE-07-2022-0137

[6] Pham TL, Zhuang XJ, Nguyen THT, Nguyen PA, Trinh DT, Do TQ. 3D printable concrete: Mixture design and laboratory test methods. Minist Sci Technol Vietnam. 2023 Mar;65(1):3-8.

[7] Liu Z, Li M, Weng Y, Wong TN, Tan MJ. Mixture Design Approach to optimize the rheological properties of the material used in 3D cementitious material printing. Constr Build Mater. 2019;198:245-55. https://doi.org/10.1016/j.conbuildmat.2018.11.252

[8] Wei Y, Tay D, Qian Y, Tan MJ. Printability region for 3D concrete printing using slump and slump flow test. Compos Part B. 2019;174:106968. https://doi.org/10.1016/j.compositesb.2019.106968
[9] Ding T, Xiao J, Zou S, Zhou X. Anisotropic behavior in bending of 3D printed concrete reinforced with fibers. Compos Struct. 2020;254:112808. https://doi.org/10.1016/j.compstruct.2020.112808
[10] Yu K, McGee W, Ng TY, Zhu H, Li VC. 3D-printable engineered cementitious composites (3DP-ECC): Fresh and hardened properties. Cem Concr Res. 2021;143:106388. https://doi.org/10.1016/j.cemconres.2021.106388
[11] Liu B, et al. Study on anisotropy of 3D printing PVA fiber reinforced concrete using destructive and non-destructive testing methods. Case Stud Constr Mater. 2022;17:e01519. https://doi.org/10.1016/j.cscm.2022.e01519
[12] Rahul AV, Santhanam M, Meena H, Ghani Z. Mechanical characterization of 3D printable concrete. Constr Build Mater. 2019;227:116710. https://doi.org/10.1016/j.conbuildmat.2019.116710
[13] Nguyễn VT. The effect of printing direction on strength of 3D printed concrete. J Mater Constr. 2022 Dec;12(2):4-12. https://doi.org/10.54772/jomc.v12i02.355
[14] Lyu X, et al. Mechanical performance and anisotropic analysis of rubberised 3D-printed concrete incorporating PP fibre. Environ Sci Pollut Res. 2024 Jul;31(36):49100-15. https://doi.org/10.1007/s11356-024-34437-w
[15] Ye J, Cui C, Yu J, Yu K, Dong F. Effect of polyethylene fiber content on workability and mechanical-anisotropic properties of 3D printed ultra-high ductile concrete. Constr Build Mater. 2021 Apr;281:122586. https://doi.org/10.1016/j.conbuildmat.2021.122586
[16] Nan B, Qiao Y, Leng J, Bai Y. Advancing Structural Reinforcement in 3D-Printed Concrete: Current Methods, Challenges, and Innovations. Materials (Basel). 2025;18(2). https://doi.org/10.3390/ma18020252
[17] Zhou Y, Althoey F, Alotaibi BS, Gamil Y, Iftikhar B. An overview of recent advancements in fibre-reinforced 3D printing concrete. Front Mater. 2023;10:1-20. https://doi.org/10.3389/fmats.2023.1289340
[18] Manikandan K, Wi K, Zhang X, Wang K, Qin H. Characterizing cement mixtures for concrete 3D printing. Manuf Lett. 2020;24:33-7. https://doi.org/10.1016/j.mfglet.2020.03.002
[19] Salim AM, Salim AM. Mechanical Properties of Different Types of Fiber-Reinforced Concrete: Benefits and Limitations. Proc Int Struct Eng Constr. 2024;11(2):1-6. https://doi.org/10.14455/ISEC.2024.11(2).MAT-09
[20] Shafei B, Kazemian M, Dopko M, Najimi M. State-of-the-art review of capabilities and limitations of polymer and glass fibers used for fiber-reinforced concrete. Materials (Basel). 2021;14(2):1-45. https://doi.org/10.3390/ma14020409
[21] Mehrabi P, Dackermann U, Siddique R, Rashidi M. A Review on the Effect of Synthetic Fibres, Including Macro Fibres, on the Thermal Behaviour of Fibre-Reinforced Concrete. Buildings. 2024;14(12). https://doi.org/10.3390/buildings14124006
[22] Kabir SMF, Mathur K, Seyam AFM. A critical review on 3D printed continuous fiber-reinforced composites: History, mechanism, materials and properties. Compos Struct. 2020;232:111476. https://doi.org/10.1016/j.compstruct.2019.111476
[23] Ministry of Science and Technology. TCVN 10302:2014. Activity admixture - Fly ash for concrete, mortar and cement. Hanoi; 2014.
[24] Duc PT. Research on using original fly ash of Hai Phong thermal power plant as a mineral additive to improve the properties of large concrete blocks. Hai Phong; 2019.
[25] Honghe G. Produc Factory Inspection Report: Polyethylene Fiber. Shandong, China; 2023.
[26] Honghe G. Produc Factory Inspection Report: High Molecular Polyethylene Fiber. Shandong, China; 2023.
[27] Rahman M, Rawat S, Yang R, Mahil A, Zhang YX. A comprehensive review on fresh and rheological properties of 3D printable cementitious composites. J Build Eng. 2024;91:109719. https://doi.org/10.1016/j.jobe.2024.109719
[28] Zhang C, Hou Z, Chen C, Zhang Y, Mechtcherine V, Sun Z. Design of 3D printable concrete based on the relationship between flowability of cement paste and optimum aggregate content. Cem Concr Compos. 2019;104:103406. https://doi.org/10.1016/j.cemconcomp.2019.103406
[29] Ministry of Science and Technology. TCVN 3119:2022. Hardened concrete - Test method for flexural tensile strength. Hanoi; 2022.
[30] Bộ Khoa học và Công nghệ. TCVN 3121-11:2022. Vữa xây dựng - Phương pháp thử. Phần 11: Xác định cường độ uốn và nén của vữa đóng rắn. 2022.
[31] Engineering Center at Iowa State University. Fiber-Reinforced Concrete for Bridge Decks Final Report. No. October. 2021. [Online].

[32] Plizzari G, Mindess S. Fiber-reinforced concrete. In: Developments in the Formulation and Reinforcement of Concrete. Elsevier; 2019. p. 257-87. https://doi.org/10.1016/B978-0-08-102616-8.00011-3
[33] Ding T, Xiao J, Zou S, Wang Y. Hardened properties of layered 3D printed concrete with recycled sand. Cem Concr Compos. 2020 Oct;113:103724. https://doi.org/10.1016/j.cemconcomp.2020.103724
[34] Wolfs RJM, Bos FP, Salet TAM. Hardened properties of 3D printed concrete: The influence of process parameters on interlayer adhesion. Cem Concr Res. 2019;119:132-40. https://doi.org/10.1016/j.cemconres.2019.02.017
[35] Liu K, Takasu K, Jiang J, Zu K, Gao W. Mechanical properties of 3D printed concrete components: A review. Dev Built Environ. 2023;16:100292. https://doi.org/10.1016/j.dibe.2023.100292
[36] Du G, Qian Y. Effects of printing patterns and loading directions on fracture behavior of 3D printed Strain-Hardening Cementitious Composites. Eng Fract Mech. 2024 Jun;304:110155. https://doi.org/10.1016/j.engfracmech.2024.110155
[37] Zeng JJ, Hu X, Sun HQ, Liu Y, Chen WJ, Zhuge Y. Triaxial compressive behavior of 3D printed PE fiber-reinforced ultra-high performance concrete. Cem Concr Compos. 2025 Jan;155:105816. https://doi.org/10.1016/j.cemconcomp.2024.105816
[38] Mohd Radzuan NA, Mohd Foudzi F, Sulong AB, Furjan M. Comprehending the effect of printing orientation on the mechanical performance of polyamide-reinforced carbon fibre composites. Compos Adv Mater. 2025 Nov;34:1-9. https://doi.org/10.1177/26349833241302492
[39] İlcan H, Özkılıç H, Tuğluca MS, Şahmaran M. Interlayer mechanical performance of 3D-printed cementitious systems: A comprehensive study on operational and material parameters. Constr Build Mater. 2024 Mar;419:135463. https://doi.org/10.1016/j.conbuildmat.2024.135463